

Ether phospholipids are required for mitochondrial reactive oxygen species homeostasis

List of Supplementary Information

Supplementary Figures

Supplementary Figure 1. Sensitivity of PDAC PDX lines to different mitochondrial inhibitors.

Supplementary Figure 2. Mitochondrial complex I inhibition in PDAC PDX cells grown in glucose-rich or -limited condition.

Supplementary Figure 3. Sensitivity comparison to complex I inhibition in PDX cells grown in galactose medium or hypoxic condition.

Supplementary Figure 4. Differential responses of PDAC PDX models to treatment with mitochondrial complex I inhibitor IACS-010759.

Supplementary Figure 5. Sensitivity of PDAC PDX tumors to treatment with mitochondrial complex I inhibitor.

Supplementary Figure 6. Comparison of mitochondrial quality and quantity in complex I inhibition-sensitive and -resistant lines.

Supplementary Figure 7. Mitochondrial ROS accumulation was happened earlier than IACS-010759 induced cell death in sensitive lines.

Supplementary Figure 8. Two pH-stable GFP probes for hydrogen peroxide monitor mitochondrial localized-ROS and cytosol localized-ROS.

Supplementary Figure 9. Mitochondrial ROS induction increases cell sensitivity to IACS-010759.

Supplementary Figure 10. Higher TCA cycle components in resistant group.

Supplementary Figure 11. MUFAs and PUFAs exhibit opposite contribution to cell survival and ROS homeostasis upon mitochondrial complex I inhibition.

Supplementary Figure 12. Complex I inhibition induces lipid peroxidation in cells sensitive to IACS-010759 treatment.

Supplementary Figure 13. A deep dissection of cell death mechanism induced by IACS-010759.

Supplementary Figure 14. Blocking de novo ether phospholipid synthesis by knocking out key ether lipids generation enzymes.

Supplementary Figure 15. Supplementation with C18:1-linked ether lipids (O-C16-18:1 PC) induce accumulation in mitochondria.

Supplementary Figure 16. Peroxisome activities comparison between sensitive and resistant lines.

Supplementary Figure 17. GNPAT-deleted tumors with IACS-010759 increased cell death and lipids peroxidation.

Supplementary Figure 18. MUFA-linked ether phosphatidylcholine promotes resistance to mitochondrial complex I inhibition.

Supplementary Figure 19. MUFA-linked ether phosphatidylcholine rescue cell death induced by mitochondrial complex I inhibitor phenformin.

Supplementary Figure 20. Blue native PAGE and In-gel activity protocols identified mitochondrial supercomplexes.

Supplementary Figure 21. MUFA-linked ether phosphatidylcholine promotes the formation of high-molecular-weight supercomplexes.

Supplementary Figure 22. Decrease to SCs assembly by knocking out UQCC3 sensitize to complex I inhibition.

Supplementary Tables

Supplementary Table 1. IC50 for IACS-010759 in PDXs.

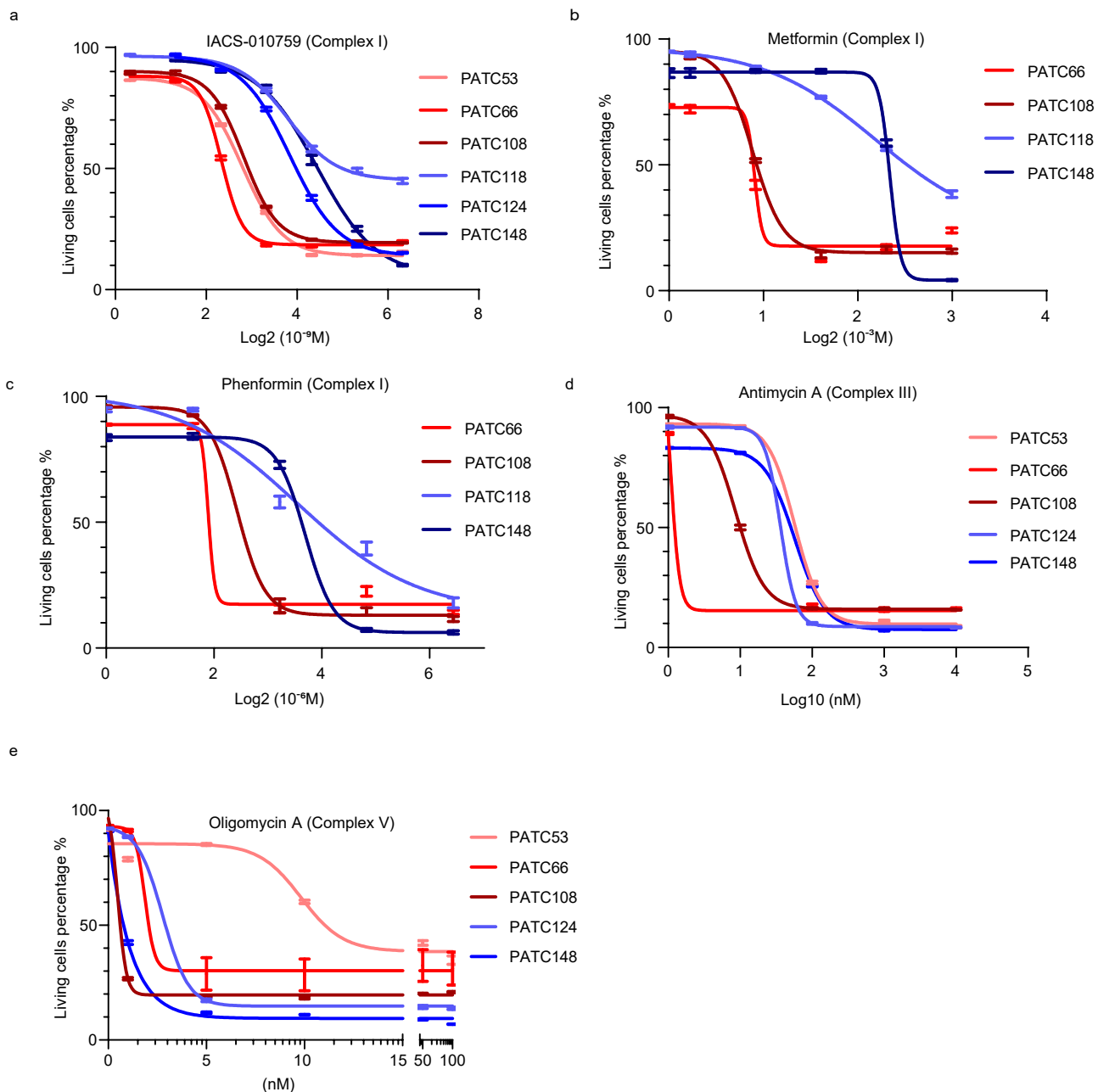
Supplementary Table 2. Main genetic mutation features in PDXs.

Supplementary Data

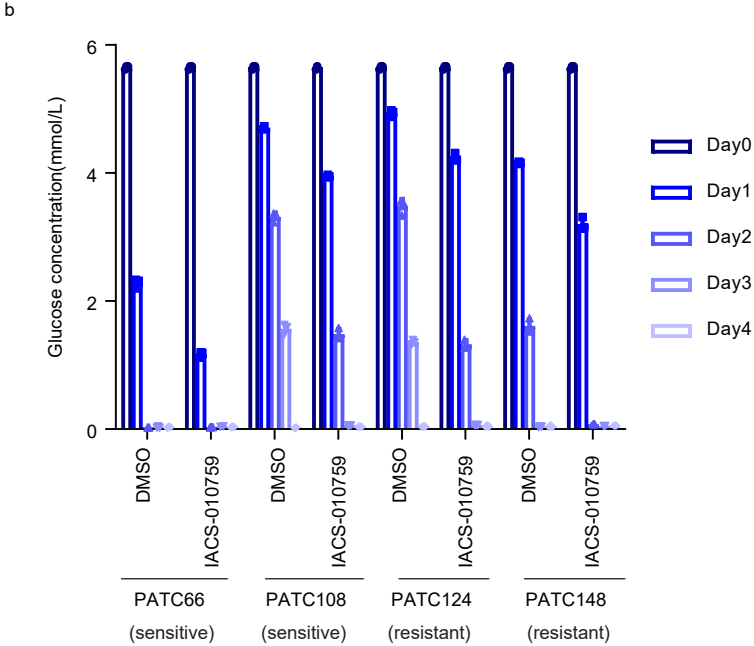
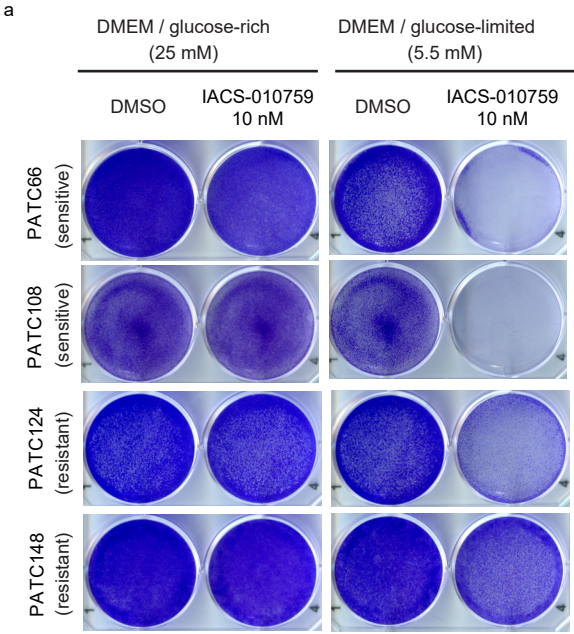
Supplementary Data 1. Global polar metabolomics in PDX lines.

Supplementary Data 2. Whole cell lipidomics in PDX lines.

Supplementary Data 3. Lipidomics in purified mitochondria of PDX lines.

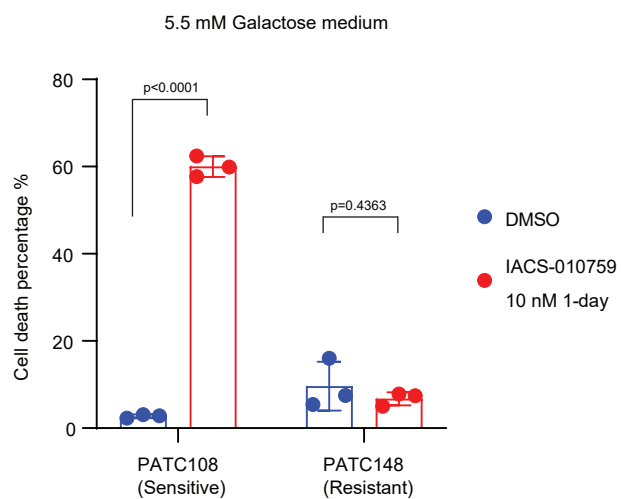


Supplementary Figure 1. Sensitivity of PDAC PDX lines to different mitochondrial inhibitors. Dose-response curves in representative PATC lines grown in 5.5 mM glucose and treated for 72 hours with complex I inhibitors IACS-010759 (a), metformin (b), phenformin (c), or complex III inhibitor antimycin A (d), or complex V inhibitor oligomycin A (e) at the indicated concentration. Cell death was detected by propidium iodide staining and flow cytometry. Data represent mean \pm S.D of 3 biologically independent replicates (a-e).

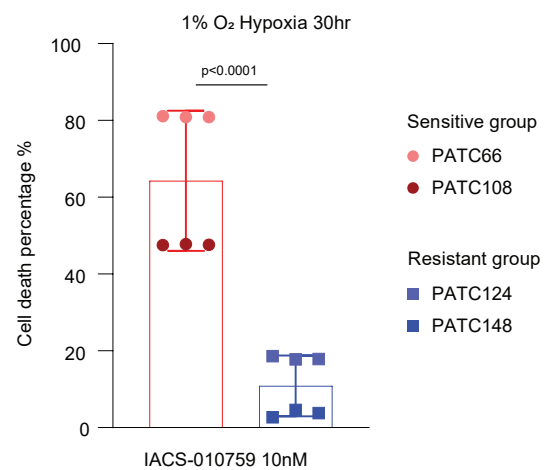


Supplementary Figure 2. Mitochondrial complex I inhibition in PDAC PDX cells grown in glucose-rich or -limited condition. a) Crystal violet staining of cells grown in the presence or absence of 10nM IACS-010759 in 25 mM or 5.5 mM glucose for 4 days. b) Medium glucose concentration was detected in sensitive lines (PATC66/108) and resistant lines (PATC124/148) with DMSO or 10 nM IACS-010759 treatment for 0, 1, 2, 3, 4-days. Data represent mean \pm S.D of 3 biologically independent replicates.

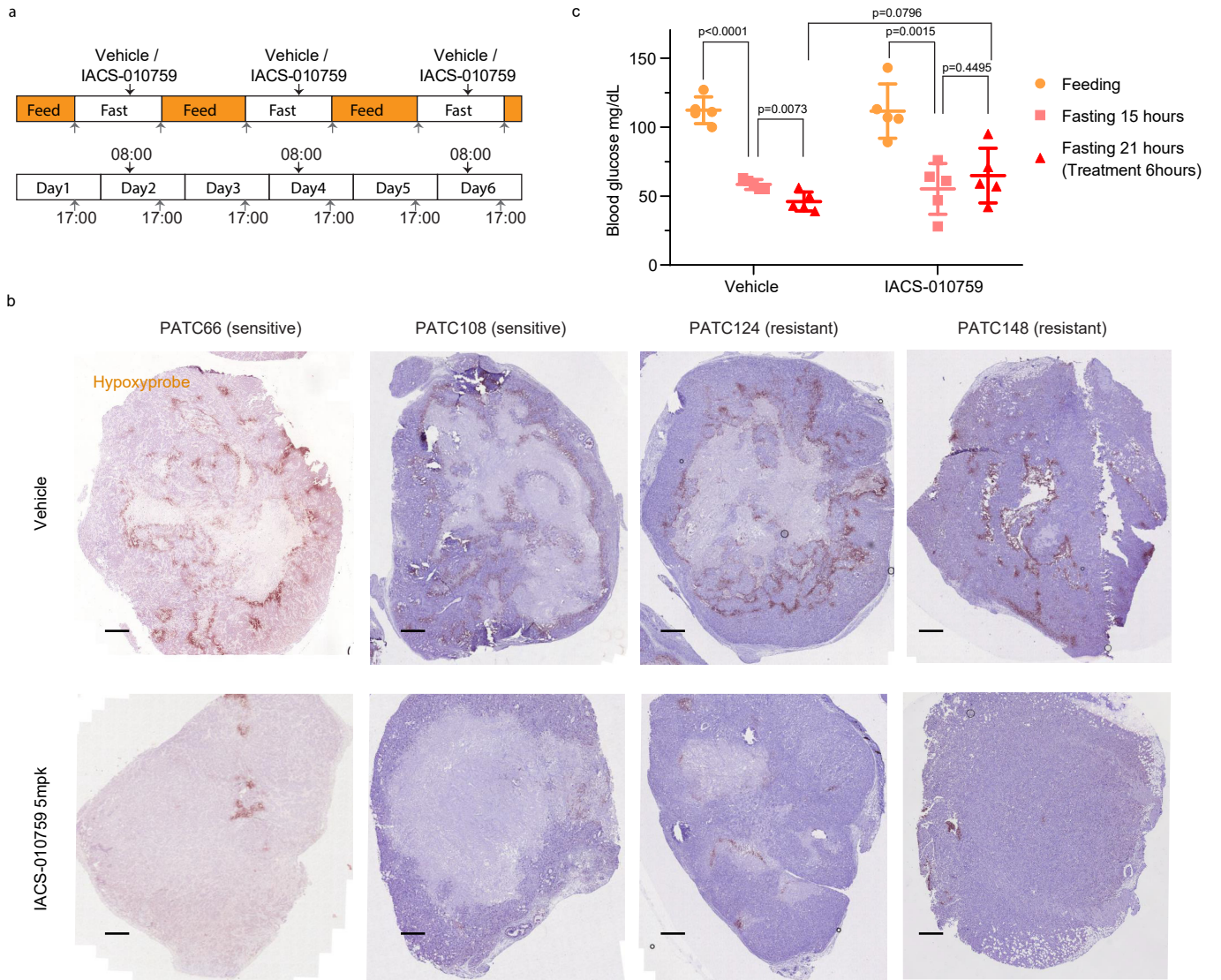
a



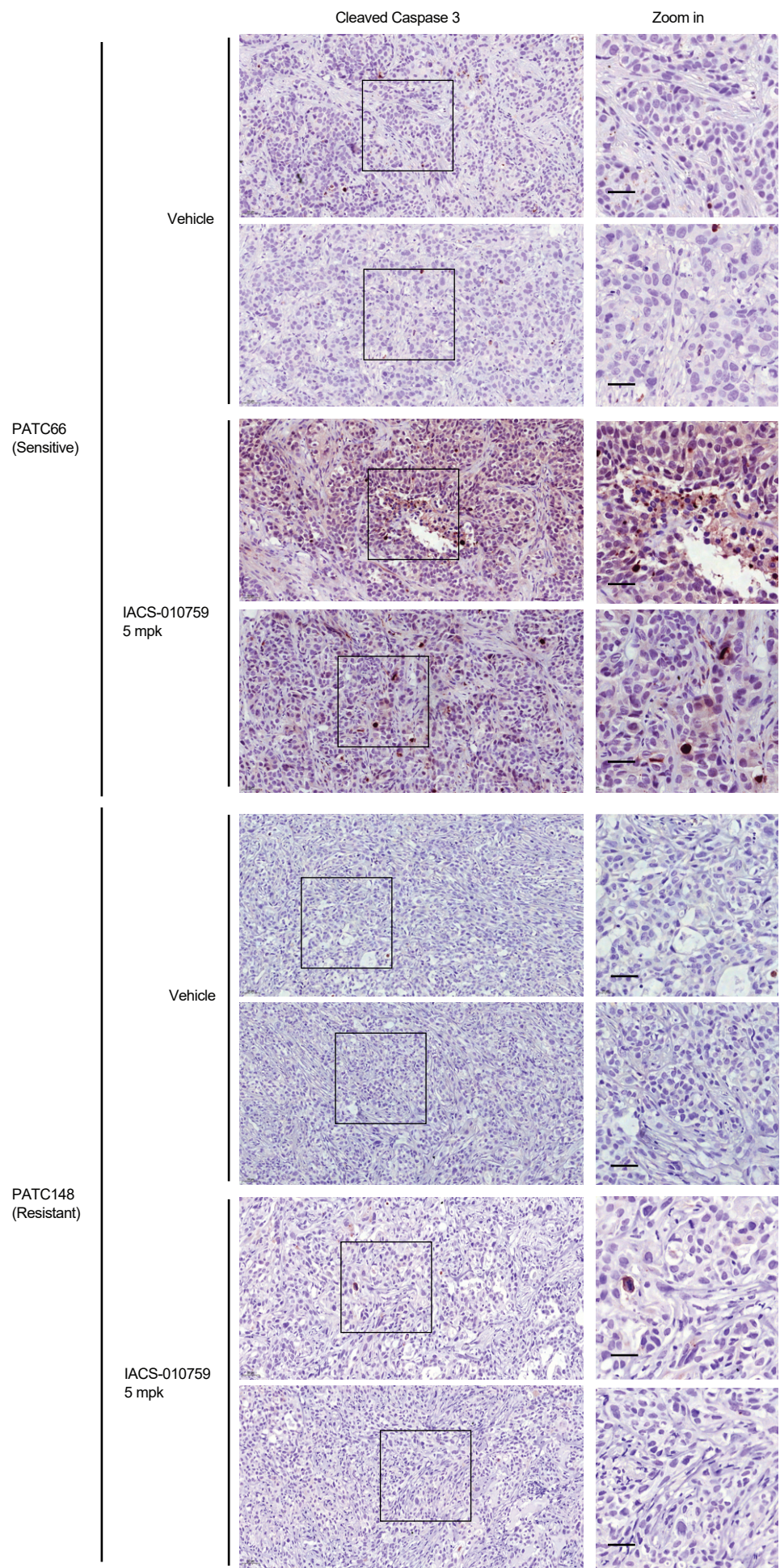
b



Supplementary Figure 3. Sensitivity comparison to complex I inhibition in PDX cells grown in galactose medium or hypoxic condition. a) PATC108 (sensitive) and PATC148 (resistant) cells were treated with DMSO or 10 nM IACS-010759 for 1-day in 5.5 mM galactose medium. Cell viability were detected by PI stain. Data represent mean \pm S.D of 3 biologically independent replicates. b) Cell viability assay assessing response of sensitive (PATC66/108) and resistant (PATC124/148) PDX lines to IACS-010759 (10 nM) for 30 hours under hypoxic conditions (1% O₂). 3 biologically independent replicates per cell line. Data represent mean \pm S.D between sensitive group (2 cell lines) and resistant group (2 cell lines). Statistical analysis by two-tailed Students' unpaired t test with significance indicated (a, b). Source data are provided as a Source Data file.

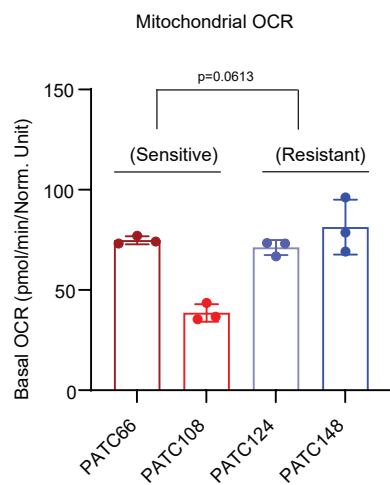


Supplementary Figure 4. Differential responses of PDAC PDX models to treatment with mitochondrial complex I inhibitor IACS-010759. a) Schematic representation of fasting/feeding protocols and timing of IACS-010759 administration in the PDX models. b) Representative IHC images showing hypoxia (Hypoxyprobe, pimonidazole) staining of PATCs xenograft tumors, from mice treated with vehicle or 5 mg/kg IACS-010759 at the 15th day. (scale bar = 500 μ m). c) Blood glucose level were monitored at the indicated times upon feeding or fasting, in mice treated with vehicle or 5mg/kg IACS-010759 once every other day. Data represent mean \pm S.D of 5 biologically independent replicates. Statistical analysis by two-tailed Students' unpaired t test with significance indicated (c). Source data are provided as a Source Data file.

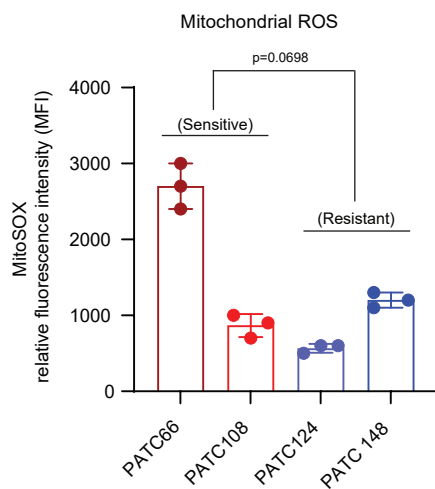


Supplementary Figure 5. Sensitivity of PDAC PDX tumors to treatment with mitochondrial complex I inhibitor. Representative IHC for cleaved caspase 3 activity in PATC subcutaneous tumors treated with vehicle or 5mg/kg IACS-010759 on the 23rd (PATC66) and 26th (PATC148) days. For each treatment, 2 independent tumors were stained. Scale bar, 50 μ m.

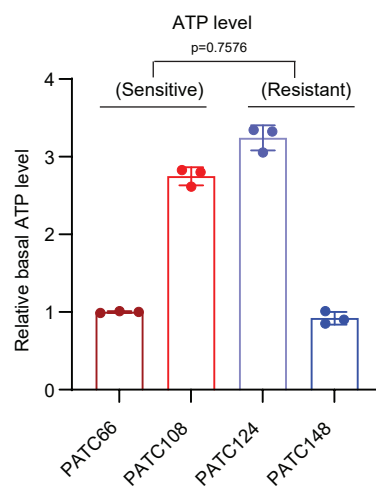
a



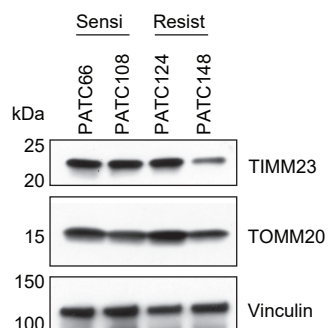
b



c



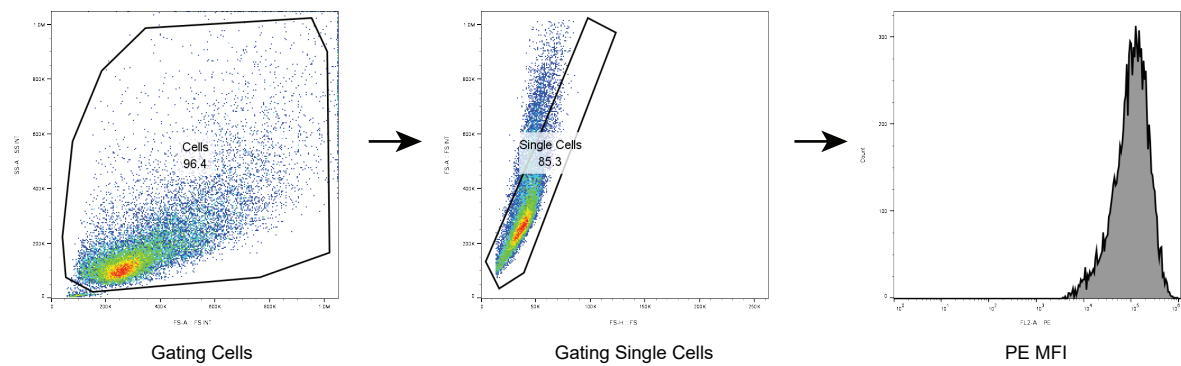
d



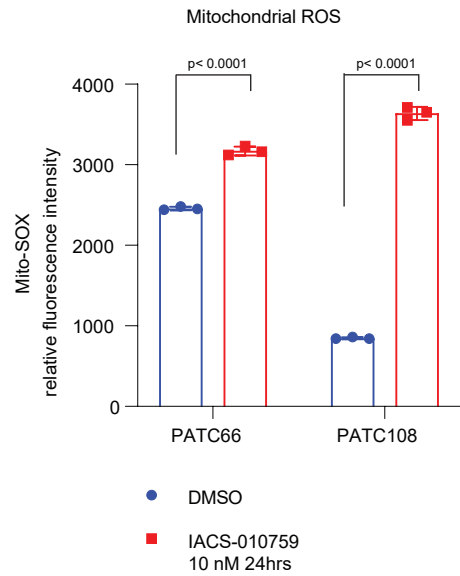
Supplementary Figure 6. Comparison of mitochondrial quality and quantity in complex I inhibition-sensitive and -resistant lines. Comparison of Basal oxygen consumption ratio (a), mitochondrial ROS by mito-SOX stain (b) and ATP level (c) in PATC66 / PATC108 / PATC124 / PATC148 lines. Data represent mean \pm S.D of 3 biologically independent replicates. d) Western blotting showed mitochondrial mass (TIMM23, mitochondrial inner membrane protein; TOMM20, mitochondrial outer membrane protein) in sensitive (PATC66/108) and resistant (PATC124/148) cells. Statistical analysis by two-tailed Students' unpaired t test with significance indicated (a-c). Source data are provided as a Source Data file.

a

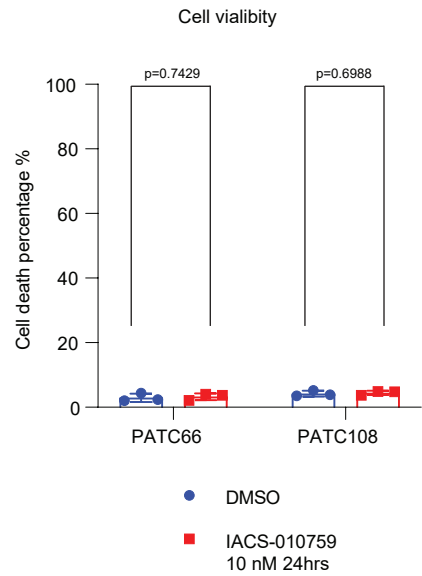
Gating strategy for flow cytometry (MitoSOX stain as an example)



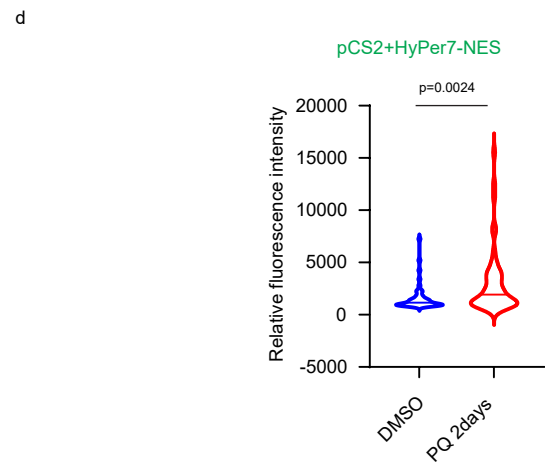
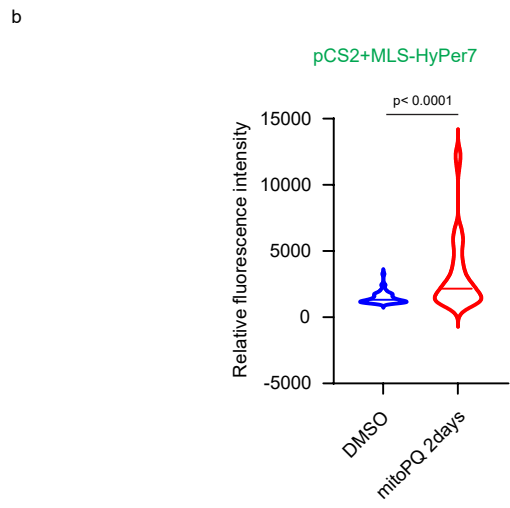
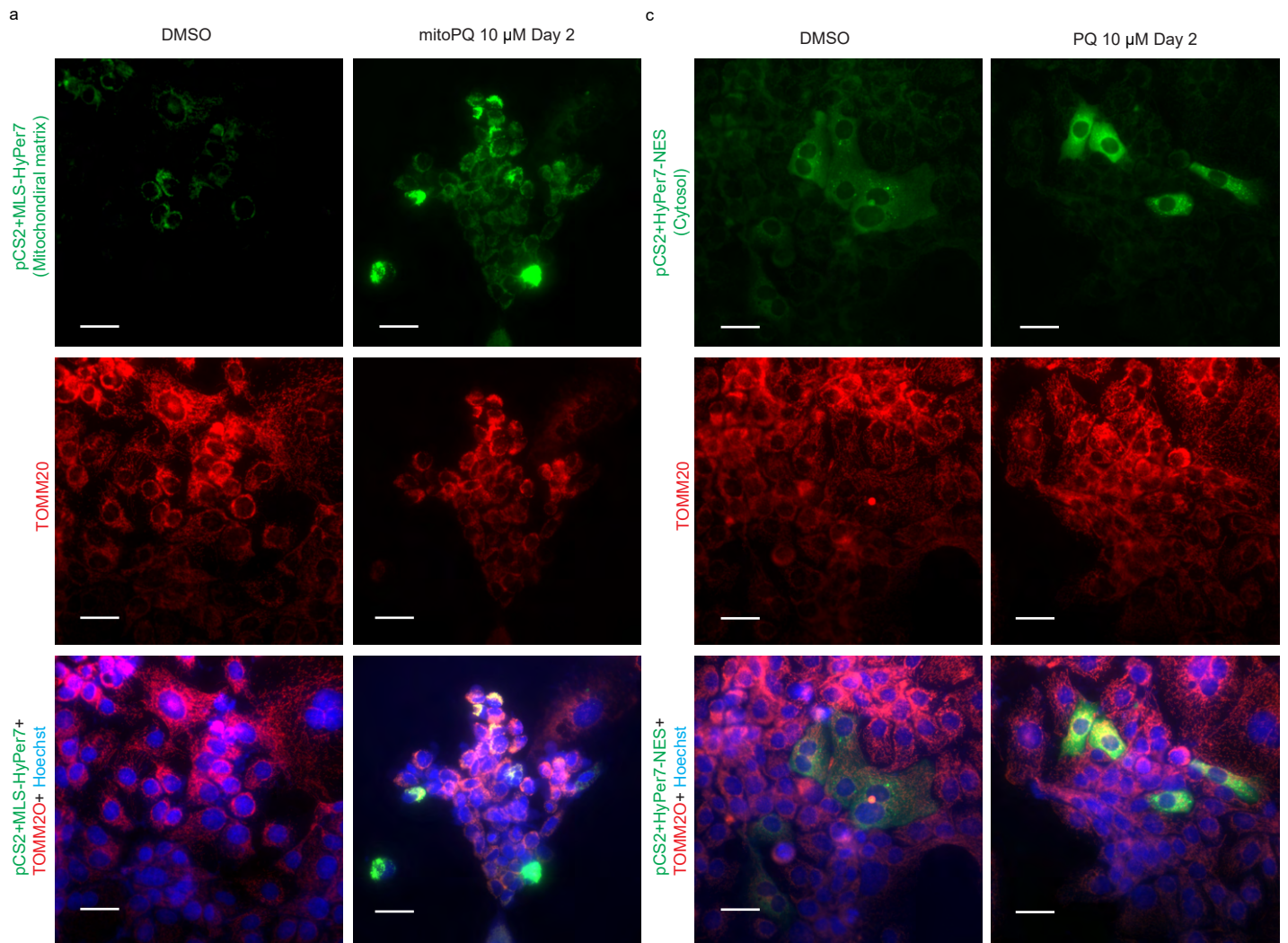
b



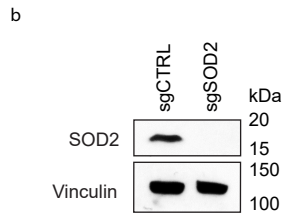
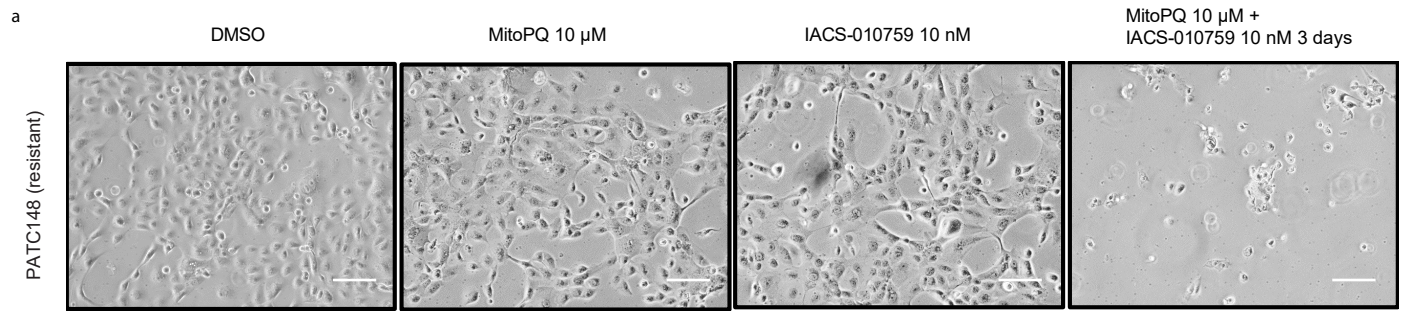
c



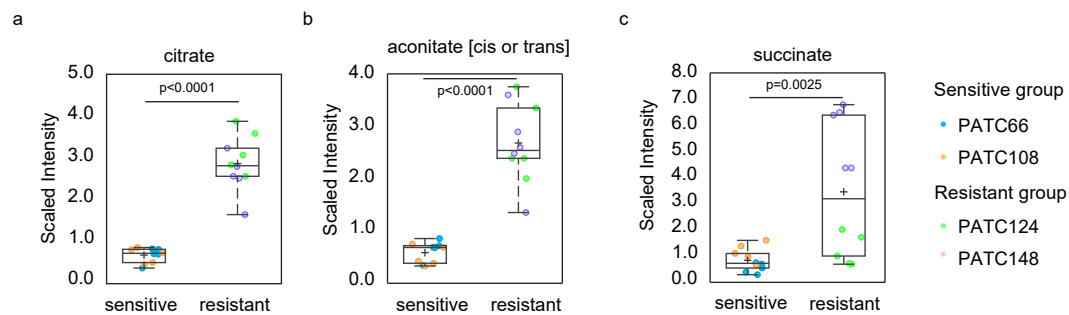
Supplementary Figure 7. Mitochondrial ROS accumulation was happened earlier than IACS-010759 induced cell death in sensitive lines. a) Flow cytometry gating strategy were used in MitoSOX data analysis. b-c) Sensitive cell lines PATC66 and 108 were treated with DMSO or 10nM IACS-010759 for 24hr. Mitochondrial ROS (b) and cell viability (c) were detected by mito-ROS and PI stain, separately. Data represent mean \pm S.D of 3 biologically independent replicates. Statistical analysis by two-tailed Students' unpaired t test with significance indicated (b, c). Source data are provided as a Source Data file.



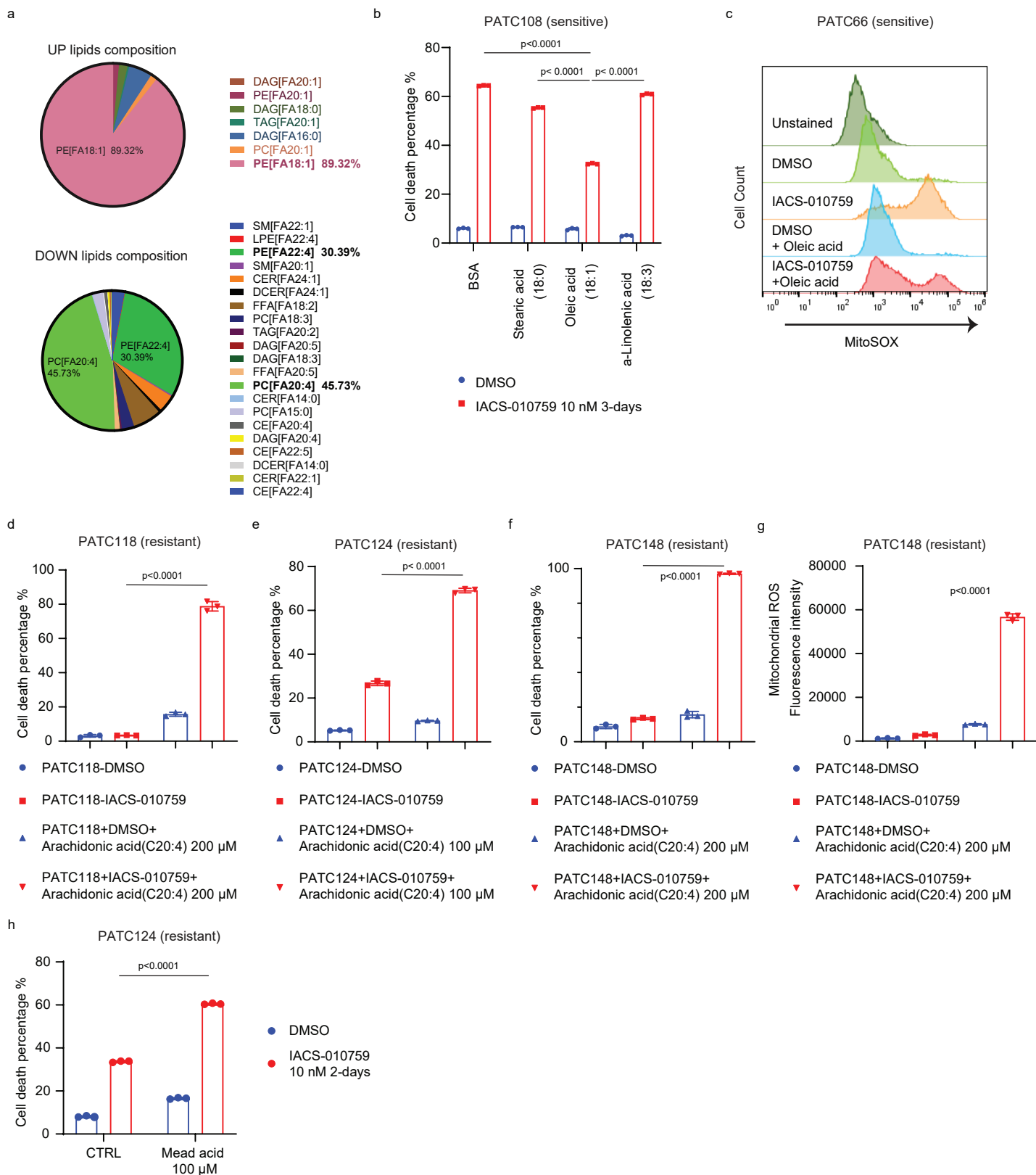
Supplementary Figure 8. Two pH-stable GFP probes for hydrogen peroxide monitor mitochondrial localized-ROS and cytosol localized-ROS. a) PATC66 cells were transfected with the hydrogen peroxide indicator pCS2+MLS-Hyper7, which is localized to the mitochondrial matrix, and treated with 10 μ M Mito-PQ or Paraquat (PQ) for 2 days. b) Quantification of fluorescence intensity in (a). At least 50 cells with positive green fluorescence were calculated for each group. c) PATC66 cells were transfected with the hydrogen peroxide indicator pCS2+HyPer7-NES, which is localized to the cytoplasm, and treated with 10 μ M Mito-PQ or PQ for 2 days. d) Quantification of fluorescence intensity in (c). At least 50 cells with positive green fluorescence were calculated for each group. For (a) and (c), mitochondria were identified with immunohistochemistry against the mitochondrial outer membrane protein, TOMM20. Nuclei were stained by Hoechst 33342. Scale bar, 30 μ m. Statistical analysis by two-tailed Students' unpaired t test with significance indicated (b, d). Source data are provided as a Source Data file.



Supplementary Figure 9. Mitochondrial ROS induction increases cell sensitivity to IACS-010759. a) Representative bright field images taken after a 3 day-treatment with 10 nM IACS-010759 with or without 10 μ M MitoPQ in PATC148. Scale bar, 50 μ m. 3 independent replicates had been done with similar results. b) Western blot with SOD2 and vinculin antibodies in PATC124 cells infected with control sgRNA (sgCTRL) or sgRNA targeting SOD2 (sgSOD2). 2 independent replicates had been done with similar results. Source data are provided as a Source Data file.

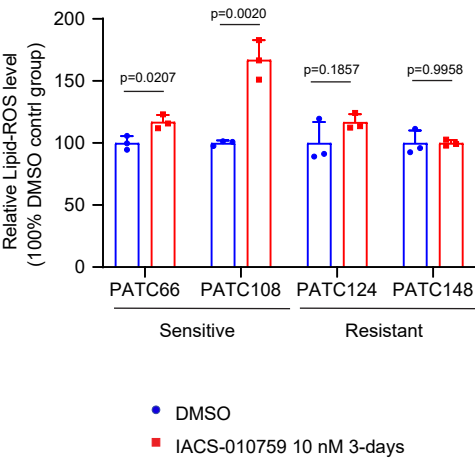


Supplementary Figure 10. Higher TCA cycle components in resistant group. a-c) Relative amounts of citrate (a), aconitate [cis or trans] (b), succinate (c) in sensitive (PATC66/108) and resistant (PATC124/148) lines. The boxes range from 25th and the 75th percentiles; Horizontal lines within box denote median value, and crosses denote mean value; whiskers denote error bars with 5% and 95% percentiles. 5 biologically independent replicates per cell line. Data represent mean \pm S.D between sensitive group (2 cell lines) and resistant group (2 cell lines). Statistical analysis by two-tailed Students' unpaired t test with significance indicated (a-c). Source data are provided as a Source Data file.

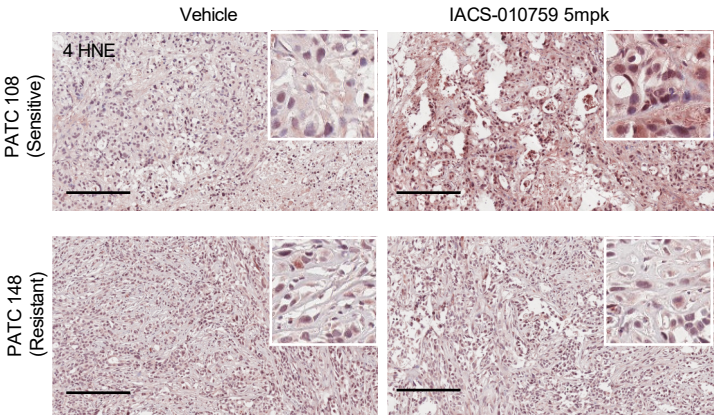


Supplementary Figure 11. MUFAs and PUFAs exhibit opposite contribution to cell survival and ROS homeostasis upon mitochondrial complex I inhibition. a) Composition of lipid species among lipids that are differentially presented in resistant versus sensitive cells. b) Cell death detected by propidium iodide staining in PATC108 cells upon DMSO or 10 nM IACS-010759 treatment in the presence of either 200 μ M stearic acid (C18:0), oleic acid (C18:1) or - Linolenic acid (C18:3), respectively. Data represent mean \pm S.D of 3 biologically independent replicates. c) Mitochondrial ROS detected by MitoSOX staining in PATC66 cells after 3 days of treatment with DMSO or 10 nM IACS-010759 in the presence or absence of 200 μ M oleic acid. d-f) Cell death in PATC118 (d), PATC124 (e), and PATC148 (f) after 3-days of treatment with DMSO or 10 nM IACS-010759, in the presence or absence of PUFA (arachidonic acid C20:4) at the indicated concentration. Data represent mean \pm S.D of 3 biologically independent replicates. g) Mitochondrial ROS were detected in PATC148 cells upon 3-days treatment with DMSO or 10 nM IACS-010759, in the presence or absence of 200 μ M PUFA (arachidonic acid C20:4). Data represent mean \pm S.D of 3 biologically independent replicates. h) PATC124 cells were treated with DMSO or 10nM IACS-010759, in the presence or absence of 100 μ M mead acid, for 2-days. Propidium iodide (PI) stain was detected for cell death events by flowcytometry. Data represent mean \pm S.D of 3 biologically independent replicates. Statistical analysis by two-tailed Students' unpaired t test with significance indicated (b, d-h). Source data are provided as a Source Data file.

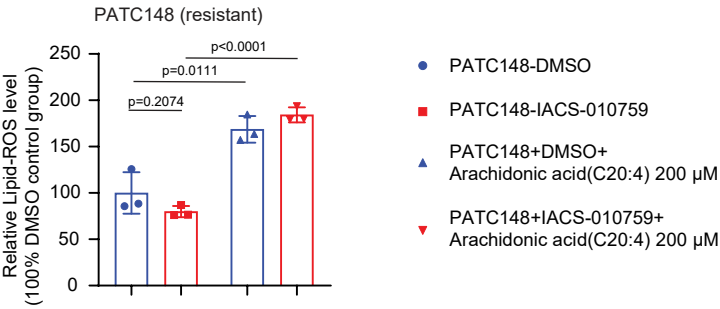
a



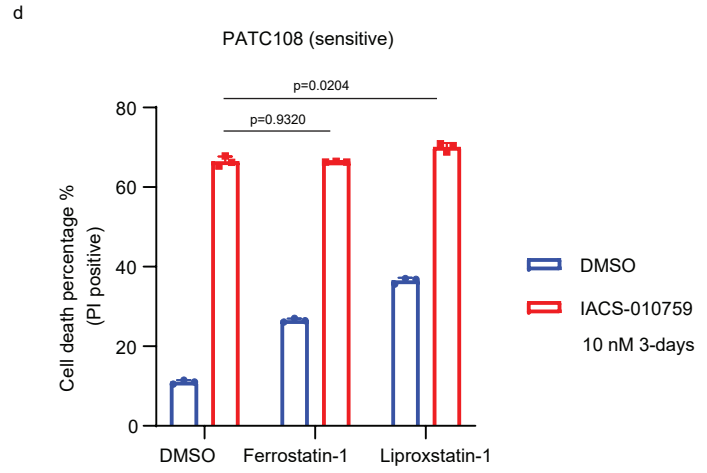
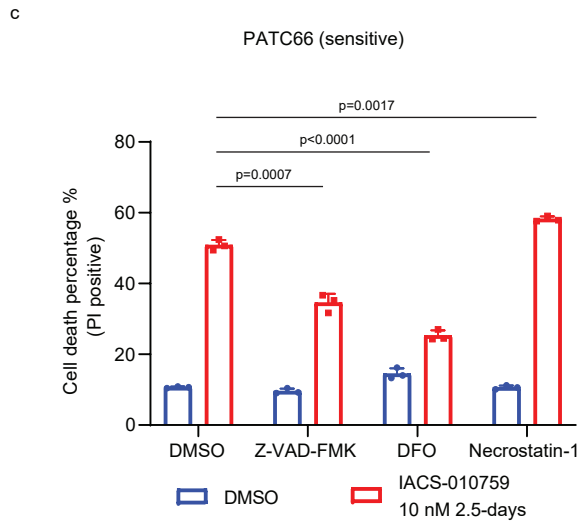
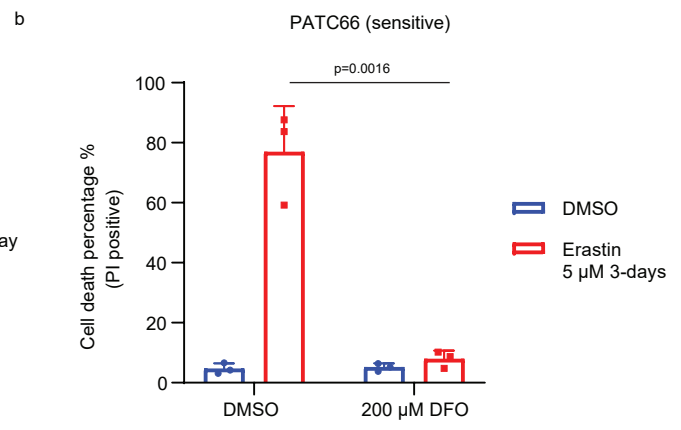
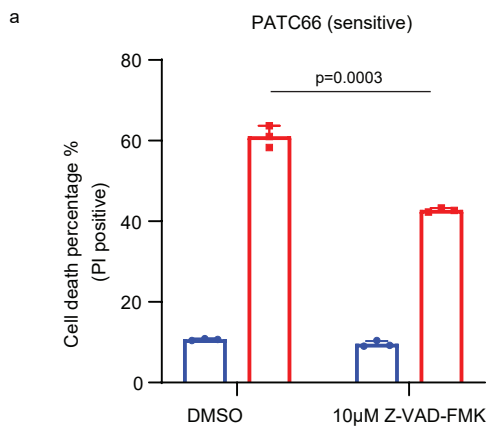
b



c

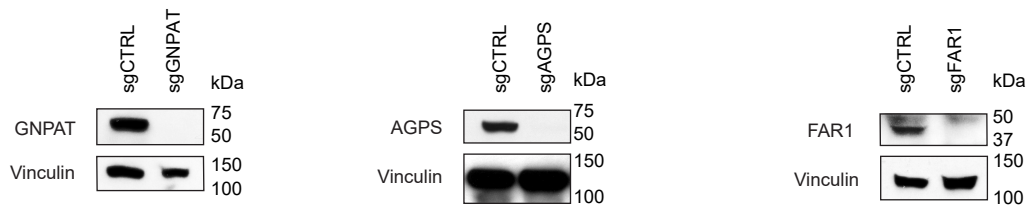


Supplementary Figure 12. Complex I inhibition induces lipid peroxidation in cells sensitive to IACS-010759 treatment. **a)** Lipid peroxidation were detected by BODIPY 581/591 C11 in complex I inhibitor-sensitive (PATC66/108) and resistant (PATC124/148) cells treated with DMSO or 10 nM IACS-010759 for 3-days. **b)** Representative 4 HNE stain in biopsies from sensitive xenograft tumor (PATC108) and resistant tumors (PATC148) in present and absent of IACS-010759 with 5 mpk, showed lipid peroxidation in vivo. Scale bar, 200 μ m. **c)** Lipid peroxidation were detected by BODIPY 581/591 C11 in complex I inhibitor resistant PATC148 cells treated with DMSO or 10 nM IACS-010759, with or without 200 μ M PUFA C20:4, for 2-days. Data represent mean \pm S.D of 3 biologically independent replicates (a, c). Statistical analysis by two-tailed Students' unpaired t test with significance indicated (a, c). Source data are provided as a Source Data file.

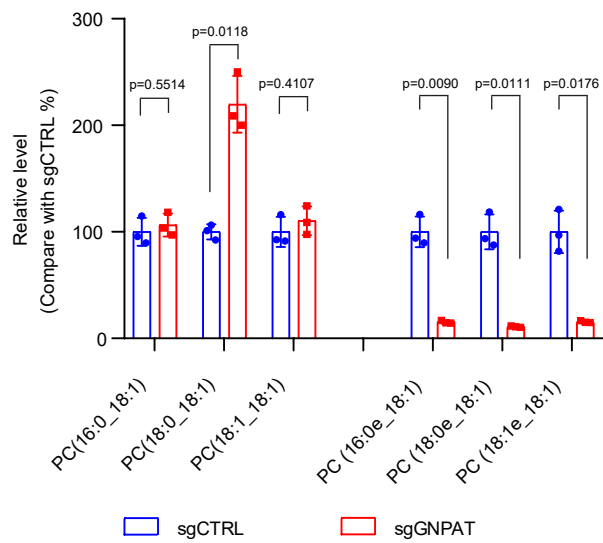


Supplementary Figure 13. A deep dissection of cell death mechanism induced by IACS-010759. a-c) PATC66 cells were treated with 0.5 $\mu\text{g/ml}$ puromycin, with or without 10 μM Z-VAD-FMK (a); 5 μM Erastin, with or without 200 μM DFO for 3-days (b), DMSO or 10 nM IACS-010759, with or without 10 μM Z-VAD-FMK, 200 μM DFO or 40 μM Necrostatin-1 for 2.5-days (c). d) PATC108 cells were treated with DMSO or 10 nM IACS-010759, with or without 10 μM Ferrostatin-1/ Liproxstatin-1 for 3-days. Flow cytometry showed PI positive cell death events. Data represent mean \pm S.D of 3 biologically independent replicates (a-d). Statistical analysis by two-tailed Students' unpaired t test with significance indicated (a-d). Source data are provided as a Source Data file.

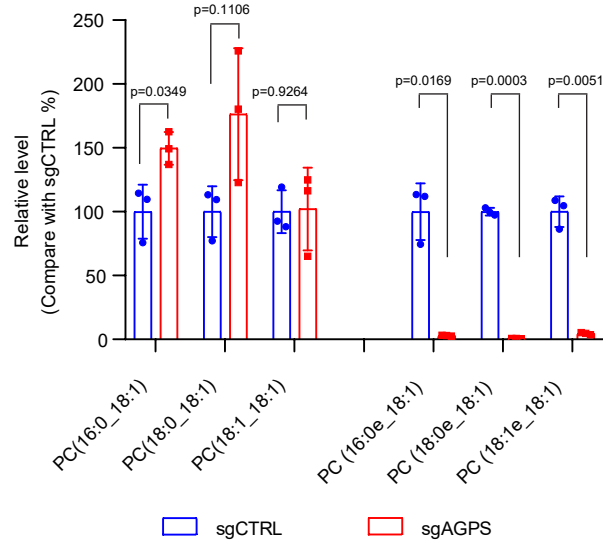
a



b

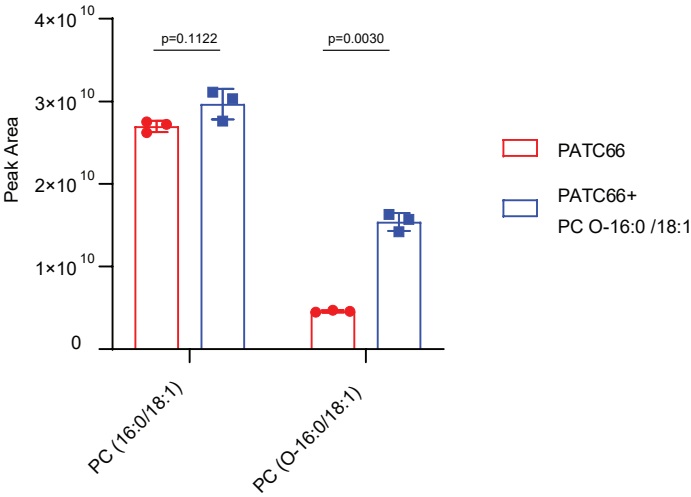


c

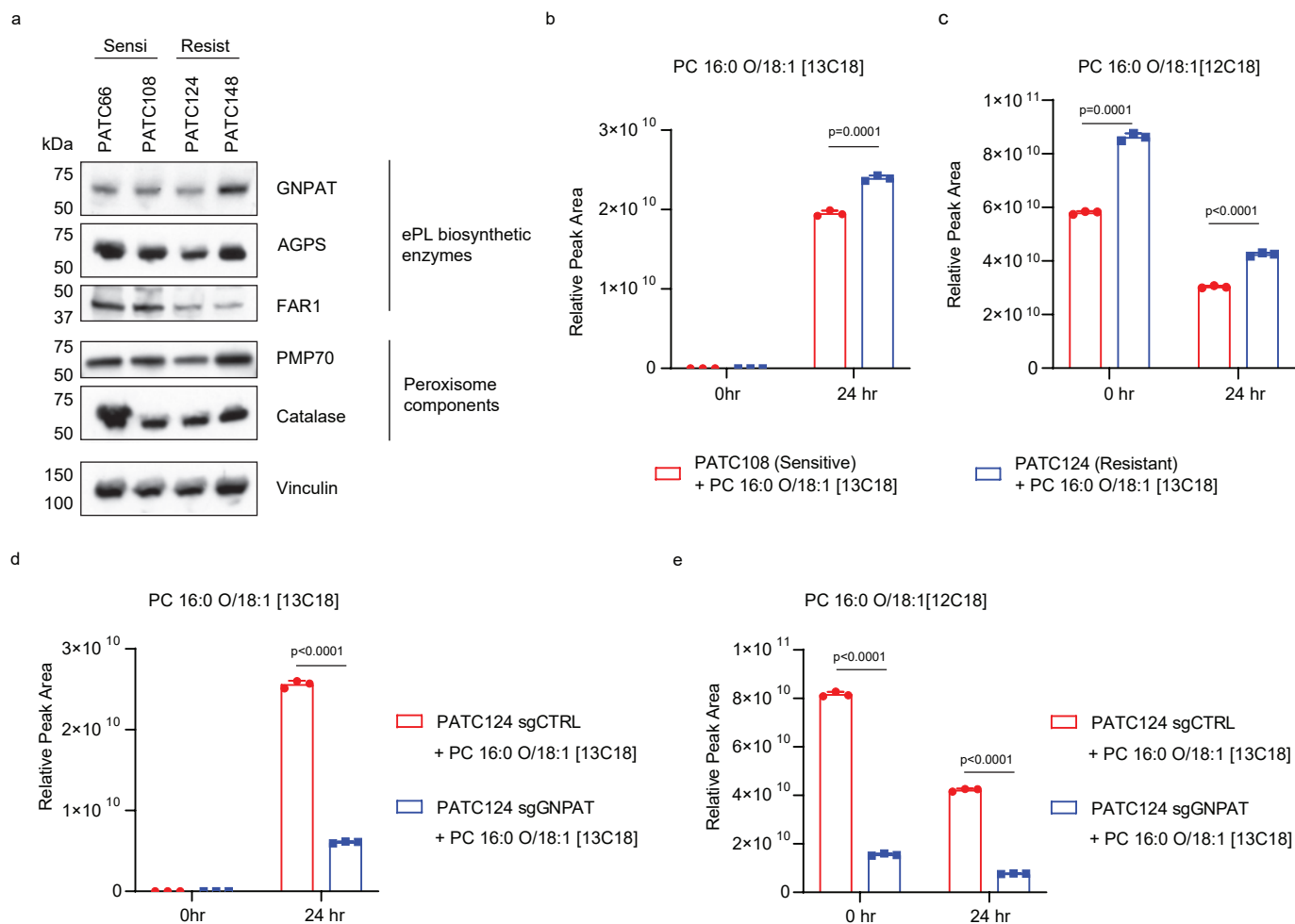


Supplementary Figure 14. Blocking de novo ether phospholipid synthesis by knocking out key ether lipids generation enzymes. a) Western blot of GNPAT, AGPS, and FAR1 in PATC124 cells infected with corresponding sgRNAs. b-c) Relative levels of indicated phospholipid or ether phospholipid in PATC124 cells infected with control sgRNA (sgCTRL), sgRNA targeting GNPAT (sgGNPAT) (b), or AGPS (sgAGPS) (c). Data represent mean \pm S.D of 3 biologically independent replicates (b, c). Statistical analysis by two-tailed Students' unpaired t test with significance indicated (b, c). Source data are provided as a Source Data file.

Exogenous PC O-16:0 /18:1 accumulation
in mitochondria

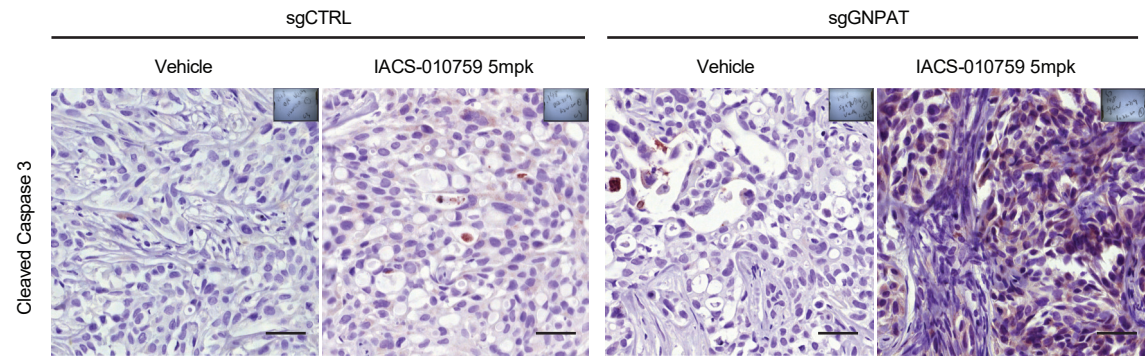


Supplementary Figure 15. Supplementation with C18:1-linked ether lipids (O-C16-18:1 PC) induce accumulation in mitochondria. a) After incubated with or without 100 μ M exogenous (O-C16-18:1 PC) for 12 hours, mitochondria from PATC66 were extracted and detected for enrichment of total PC (16:0-18:1) and ether-PC (O-16:0-18:1). Data normalized by extracted mitochondrial mass. Data represent mean \pm S.D of 3 biologically independent replicates. Statistical analysis by two-tailed Students' unpaired t test with significance indicated. Source data are provided as a Source Data file.

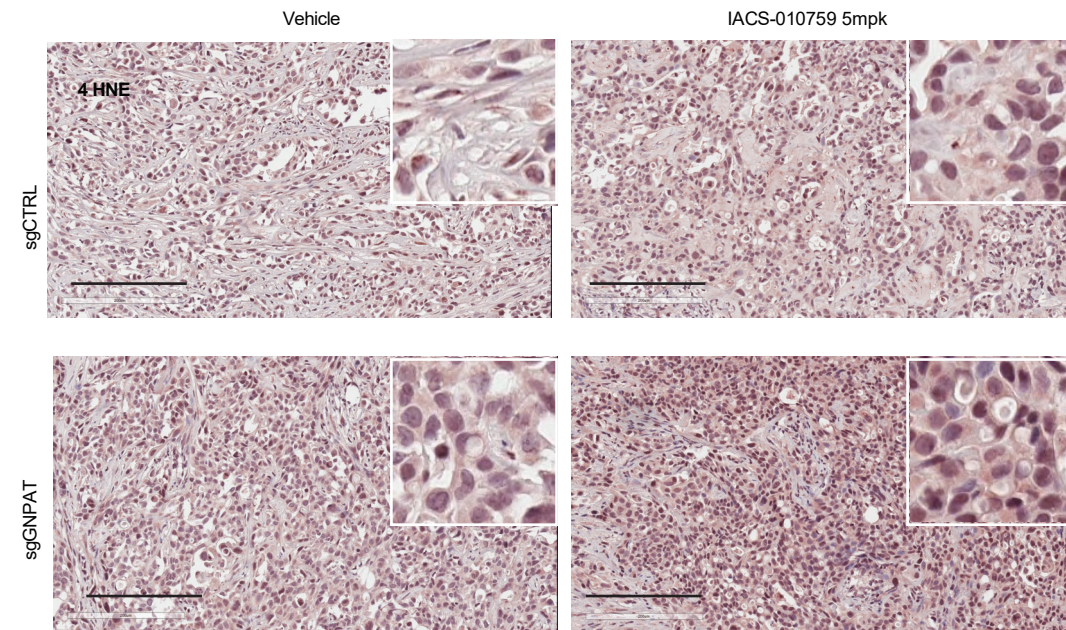


Supplementary Figure 16. Peroxisome activities comparison between sensitive and resistant lines. a) ether lipids biosynthetic enzymes (GNPAT, AGPS, FAR1) and peroxisome components (PMP70, catalase) comparison by western blotting. **b-e)** PATC108 / 124 cells (**b-c**) and PATC124 cells infected with control sgRNA (sgCTRL) or sgRNA targeting *GNPAT* (sgGNPAT) (**d-e**) were incubated with labeled oleic acid with 200 μ M ^{13}C (Oleic acid- $^{13}\text{C}_{18}$) for 1-day. The labeled / unlabeled and ether lipids (PC 16:0 O/18:1 [$^{13}\text{C}_{18}$], or PC 16:0 O/18:1 [$^{12}\text{C}_{18}$],) were detected and normalized by harvested cell number. Data represent mean \pm S.D of 3 biologically independent replicates (b-e). Statistical analysis by two-tailed Students' unpaired t test with significance indicated (b-e). Source data are provided as a Source Data file.

a

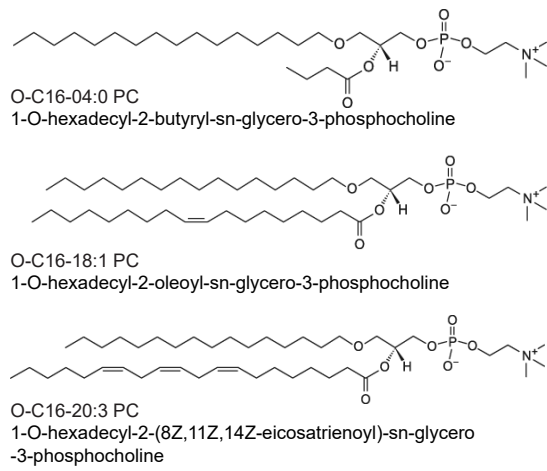


b

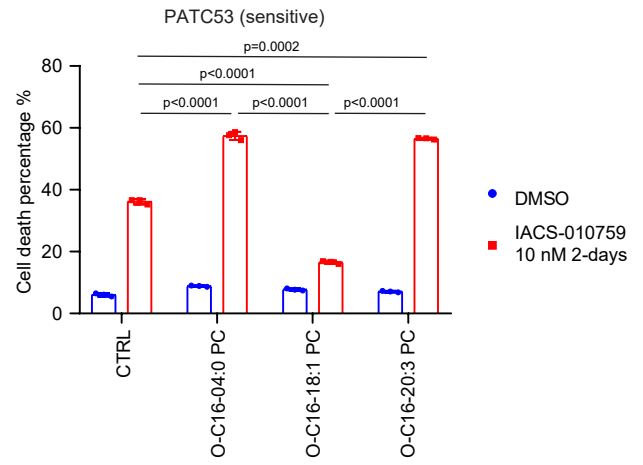


Supplementary Figure 17. GNPAT-deleted tumors with IACS-010759 increased cell death and lipids peroxidation. a) Representative IHC staining for apoptotic marker cleaved-Caspase 3 in sgCTRL/sGPNPAT PATC124 subcutaneous tumors treated with vehicle or 5 mg/kg IACS-010759. Scale bar, 50 μ m. The experiment had been repeated individually 3 times with similar results. b) Representative 4 HNE stain in biopsies from sgCTRL/sGPNPAT PATC124 xenograft tumors, in present and absent of IACS-010759 with 5 mg/kg, showed lipid peroxidation in vivo. Scale bar, 200 μ m. 3 independent replicates had been done with similar results.

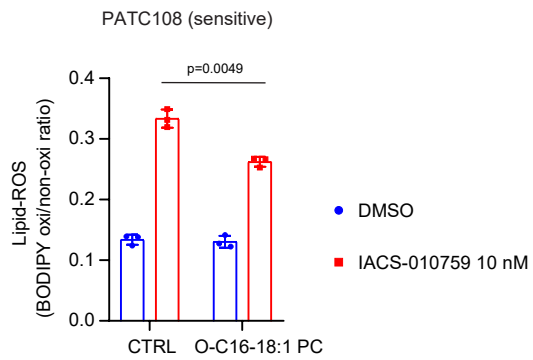
a



b

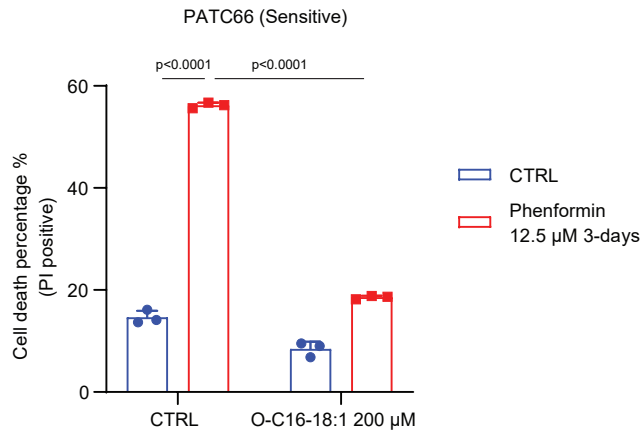


c

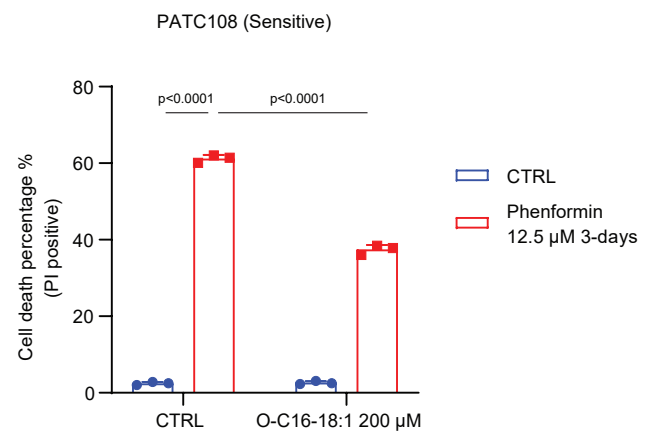


Supplementary Figure 18. MUFA-linked ether phosphatidylcholine promotes resistance to mitochondrial complex I inhibition. **a)** Structural formula of SFA (O-C16-04:0 PC), MUFA (O-C16-18:1 PC), and PUFA (O-C16-20:3 PC)-linked ether phosphatidylcholine. **b)** Cell viability was detected by propidium iodide staining and flow cytometry in PATC53 cells upon treatment with DMSO or 10 nM IACS-010759 in the presence of indicated ether phosphatidylcholine. Data represent mean \pm S.D of 3 biologically independent replicates. **c)** Lipid ROS were detected by BODIPY 581/591 C11 after a 3-day treatment with DMSO or 10 nM IACS-010759 in PATC108 cells grown in the presence or absence of 100 μ M O-C16-18:1 PC. Data represent mean \pm S.D of 3 biologically independent replicates. Statistical analysis by two-tailed Students' unpaired t test with significance indicated (b, c). Source data are provided as a Source Data file.

a

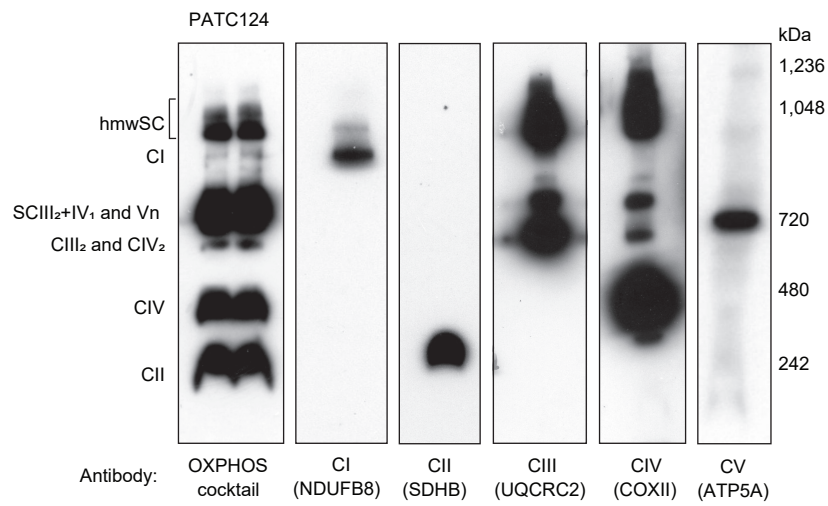


b

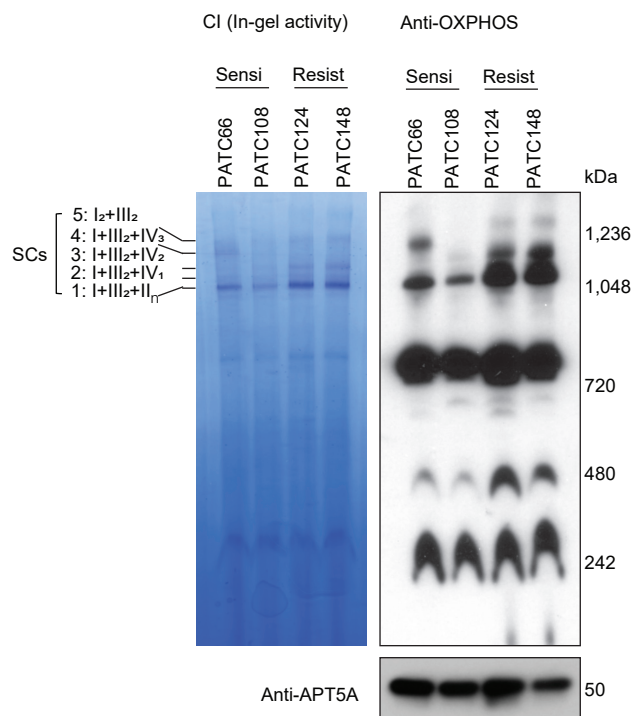


Supplementary Figure 19. MUFA-linked ether phosphatidylcholine rescue cell death induced by mitochondrial complex I inhibitor phenformin. PATC66 (a) and PATC108 (b) cells were treated with DMSO or 12.5 μ M phenformin, in the presence or absence of 200 μ M ether-MUFA O-C16-18:1, for 3-days. Propidium iodide (PI) stain was detected for cell death events by flowcytometry. Data represent mean \pm S.D of 3 biologically independent replicates. Statistical analysis by two-tailed Students' unpaired t test with significance indicated (a, b). Source data are provided as a Source Data file.

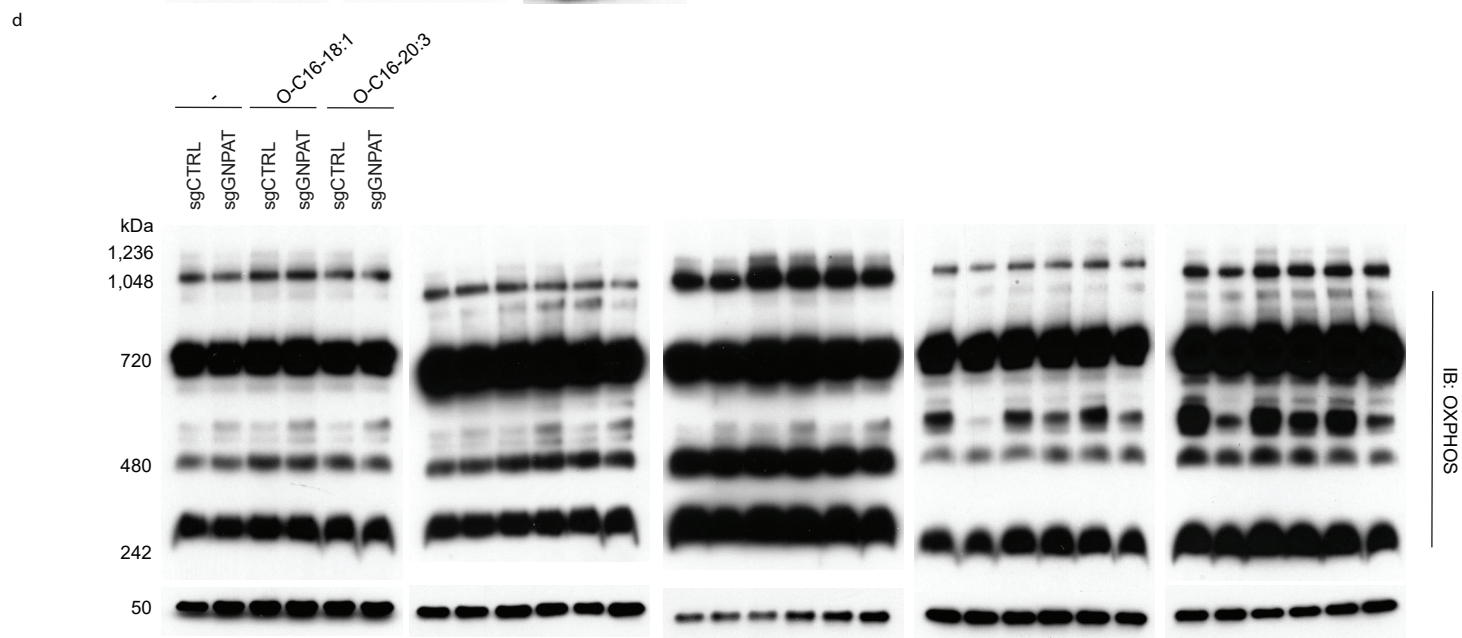
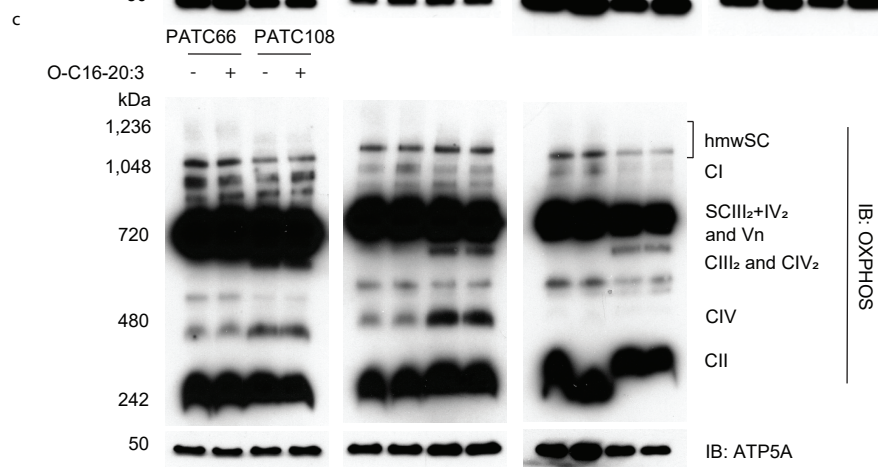
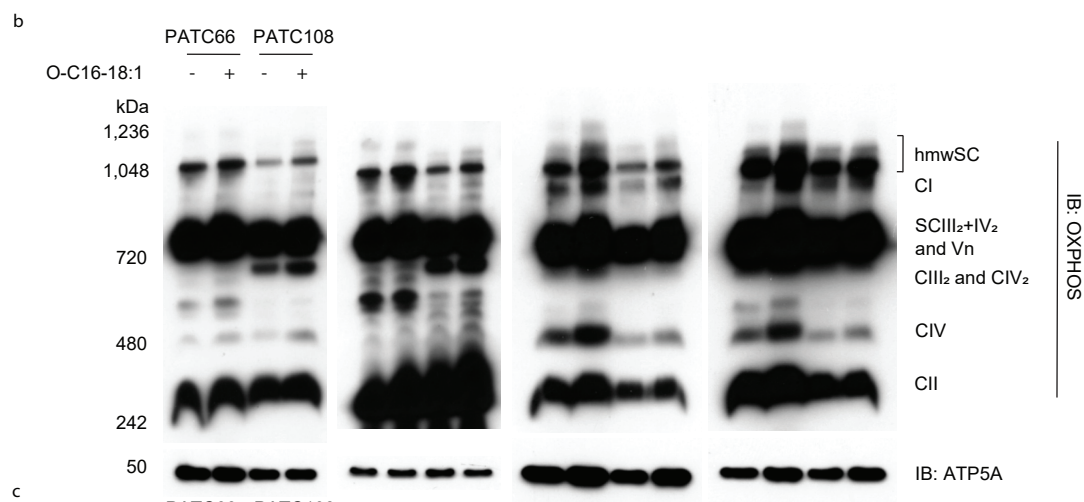
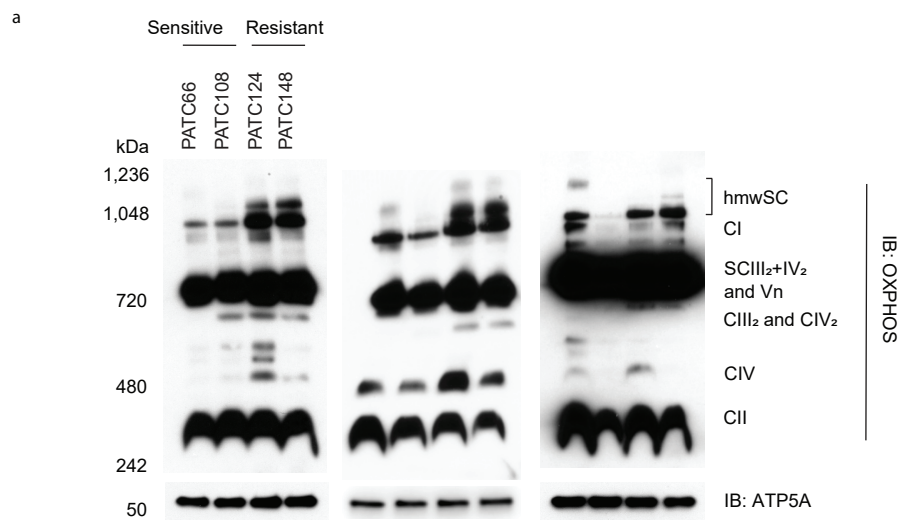
a



b

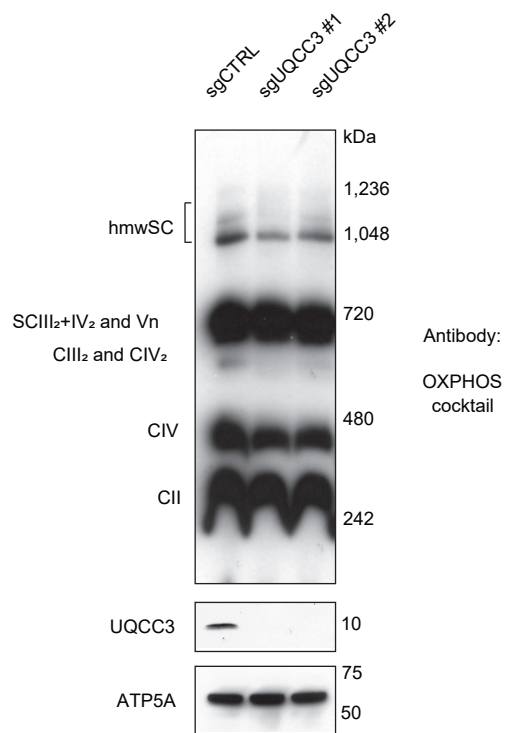


Supplementary Figure 20. Blue native PAGE and In-gel activity protocols identified mitochondrial supercomplexes. a) Mitochondrial supercomplexes (SC) were extracted in PATC124 cells and six equal samples were run with blue native PAGE in the same gel. Sample was then transferred to one PVDF membrane and divided into six parts. the six membrane parts were incubated with either an anti-OXPHOS antibody cocktail, anti-NDUFB8 antibody (Complex I targeting), anti-SDHB antibody (Complex II targeting), anti-UQCRC2 antibody (Complex III targeting), anti-COXII antibody (Complex IV targeting), or anti-ATP5A antibody (Complex V targeting). The experiment had been repeated individually 2 times with similar results. b) mitochondrial supercomplexes (SC) activity and mass in sensitive (PATC66/108) and resistant (PATC124/148) cells. 100 µg mitochondria were extracted from sensitive lines (PATC66/108) and resistant lines (PATC124/148) for BN-PAGE gel running followed by incubation with complex I substrate NADH (0.1mg/ml) for 30min in room temperature. 10% acetic acid was used to stop reaction. Supercomplexes containing complex I were showed in BN-PAGE gel with purple bands. 50 µg mitochondria were extracted for BN-PAGE blot to detect SCs mass by anti-OXPHOS and anti-ATP5A antibodies incubation. 3 independent replicates had been done with similar results.

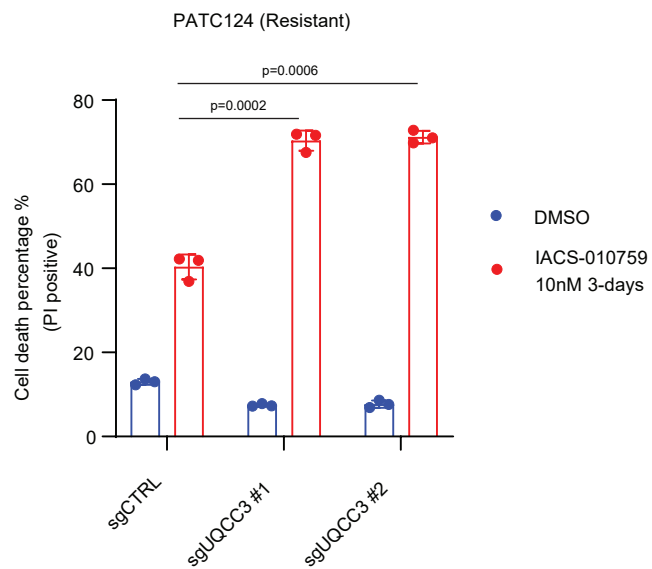


Supplementary Figure 21. MUFA-linked ether phosphatidylcholine promotes the formation of high-molecular-weight supercomplexes. a) Mitochondrial supercomplexes (SC) in PATC66 / 108 / 124 / 148 cells as shown with BN-PAGE in three independent experiments. b) Mitochondrial supercomplexes in PATC66/108 cells grown in the presence or absence of 100 μ M ether-MUFA (O-C16-18:1 phosphatidylcholin (PC)) for 24 hours. Four independent BN-PAGE results were shown. c) Mitochondrial supercomplexes in PATC66/108 cells grown in the presence or absence of 100 μ M ether-PUFA (O-C16-20:3 phosphatidylcholin (PC)) for 24 hours. Three independent BN-PAGE results were shown. d) Mitochondrial supercomplexes in PATC124 cells infected with control sgRNA (sgCTRL) or sgRNA targeting *GNPAT* (sgGNPAT) in the presence or absence of 100 μ M O-C16-18:1 PC or 100 μ M ether-PUFA (O-C16-20:3 PC) for 24 hours. 5 independent BN-PAGE results were shown.

a



b



Supplementary Figure 22. Decrease to SCs assembly by knocking out UQCC3 sensitize to complex I inhibition. a) SCs samples were extracted and components were detected in control (sgCTRL) and UQCC3 deleted PATC124 cells. b) control (sgCTRL) and UQCC3 deleted PATC124 cells were treated with DMSO or 10nM IACS-010759 for 3-days. Cell viability were detected by PI stain. Data represent mean \pm S.D of 3 biologically independent replicates. Statistical analysis by two-tailed Students' unpaired t test with significance indicated (b). Source data are provided as a Source Data file.

Supplementary Table 1. IC50 for IACS-010759 in PDXs.

	Sensitive			Resistant		
PATCs	PATC53	PATC66	PATC108	PATC118	PATC124	PATC148
IC50 (nmol/L))	6.7	5.1	7.1	13.8	13.5	20.2

Supplementary Table 2. Main genetic mutation features in PDXs.

MODEL	SNPEFF_GENE_NAME	SNPEFF_AA_CHANGE	Sensitivity to complex I
PDX-PDAC-053	KRAS	p. G12D	Sensitive PDXs
PDX-PDAC-053	TP53	p. R306*	
PDX-PDAC-066	KRAS	p. G12D	
PDX-PDAC-066	TP53	p. Y234*	
PDX-PDAC-066	CDKN2A	p. Y44fs	
PDX-PDAC-108	KRAS	p. G12D	
PDX-PDAC-108	TP53	p. R175H	
PDX-PDAC-118	KRAS	p. Q61H	Resistant PDXs
PDX-PDAC-118	TP53	p. E224D	
PDX-PDAC-118	CDKN2A	NA	
PDX-PDAC-124	KRAS	p. G12D	
PDX-PDAC-124	TP53	p. R333fs	
PDX-PDAC-124	SMAD4	NA	
PDX-PDAC-148	KRAS	p. G12D	
PDX-PDAC-148	TP53	p. F134L	